

Effects of Spin Finish on Fiber Surface Hardness: An Investigation with Atomic Force Microscopy and Frictional Measurements

Y. K. KAMATH,¹ S. B. RUETSCH,¹ E. PETROVICOVA,¹ L. KINTRUP,² H.-J. SCHWARK²

¹ TRI/Princeton, Princeton, New Jersey 08542

²Henkel KGaA, Düsseldorf, Germany

Received 5 March 2001; accepted 1 October 2001

ABSTRACT: Spin finishes are applied to melt-spun fibers to protect them from abrasion during processing. The principal component of the fiber finish is a lubricant, which generally is a random or block copolymer of ethylene oxide/propylene oxide. Although these polymers do not penetrate the fiber because of their high molecular weight, depending on the nature of the fiber polymer, they interact to cause changes in the hardness of the fiber surface. This happens to be the case with acidic polymer fibers such as nylon-6 and polyester [poly(ethylene terephthalate)], both of which are softened by the ethylene oxide/propylene oxide lubricant. We used atomic force microscopy with nanoindentation capability to study the effect of lubricants on the microhardness of nylon-6 and poly(ethylene terephthalate) fiber surfaces. Softening of the fiber surface by plasticization generally results in an increase in fiber friction because of shear deformation at the interface. We made an effort to determine the friction of fibers against a hard stainless steel surface after coating them with the finish lubricant for different lengths of time. The relevance of these results to fiber processing is discussed. © 2002 Wiley Periodicals, Inc. *J Appl Polym Sci* 85: 394–414, 2002

Key words: nylon-6 and poly(ethylene terephthalate) (PET) fibers; spin finish; lubricant/acid–base interaction; atomic force microscopy (AFM); nanoindentation; fiber friction

INTRODUCTION

Spin finishes are applied as lubricants and anti-static compounds to melt-spun fibers. The lubricant component of the spin finish is a random or block copolymer of ethylene oxide/propylene oxide (EO/PO). These copolymers, being polyethers, possess basic (electron-donating) properties, whereas fiber polymers such as nylon and poly-

ter are acidic (electron-accepting) with —COOH groups on the surface. Acid–base interactions between the finish lubricant and the fiber can lead to different degrees of plasticization of the interface, leading to softening. Such softening often gives rise to an increase in fiber–fiber and fiber–metal friction and consequent difficulties in processing. The EO/PO block copolymer may also act as an effective hydrogen-bond breaker. We used atomic force microscopy (AFM) to study changes in the hardness of fiber surfaces as a result of fiber–finish interactions.

AFM techniques are unique methods for high-resolution examinations of various materials on a

Correspondence to: Y. K. Kamath (ykamath@triprinceton.org).

Journal of Applied Polymer Science, Vol. 85, 394–414 (2002)
© 2002 Wiley Periodicals, Inc.

nanometer scale, including polymeric fibers. AFM provides information on not only the topography but also the adhesive, attractive, repulsive, viscoelastic, and micromechanical (microhardness) properties of polymeric substrates. We used AFM to study the properties of the interface between the spin finish and the fiber substrate. We made an attempt to establish finish-induced changes in the viscoelastic properties of polymeric fibers. In addition, we examined the effects of a spin finish on microroughness and the filling effect of a finish on the microroughness of the fiber surface. The principal goal of this work was to determine by the nanoindentation capability of AFM whether there was a finish-induced softening or hardening effect on the surface layer of the fiber. These studies will ultimately assist in the development of spin finishes that will cause the least amount of damage to the fiber surface and will be most beneficial in the processing of fibers.

EXPERIMENTAL

Materials

Fibers

For the nylon-6 multifilament yarn, there were 76 filaments per yarn. The fibers were spin-finish-free (water spin finish only), had a circular cross section $36\ \mu\text{m}$ in diameter, were spun and drawn at a draw ratio of 3.0, and contained no TiO_2 . The unfinished polyester multifilament yarn had a circular cross section (150-denier fully oriented yarn) about $30\ \mu\text{m}$ in diameter.

Spin Finish

The spin finish lubricant applied to the fibers was UCON HB-100, a random copolymer of EO/PO (Union Carbide Corporation, South Charleston, WV). Individual nylon-6 and poly(ethylene terephthalate) (PET) fibers as well as complete yarns were treated with the finish weeks before the study was carried out so that the finish would be able to interact with the polymer over the course of storage.

AFM Techniques

Fiber surface properties were obtained on a nanometer scale with either a NanoScope MultiMode or NanoScope Dimension scanning probe microscope from Digital Instruments (Santa Barbara,

CA) equipped with nanoindentation capabilities. Multiple AFM scanning techniques were used in this study to characterize finish-induced changes in the surface properties of nylon-6 and PET fibers. These techniques are as follows:

Topographical three-dimensional height profiles (in the tapping mode) measure topography by tapping the fiber surface with an oscillating probe tip.

Phase contrast imaging (in the tapping mode) provides contrast caused by differences in surface adhesion and viscoelasticity.

Height, phase contrast, and amplitude signals characterize the topography and morphology and measure the microroughness and total surface area.

Force–distance curves measure attractive, repulsive, and adhesive forces between the probe tip and sample during approach, contact, and separation, respectively.

Nanoindenting measures the microhardness of the fiber surface by indenting the surface with a diamond probe tip mounted on a metal-foil cantilever. The surface indentation is imaged and measured in real time.

Profile scanning analysis (also called cross-sectional analysis) measures the depth of the

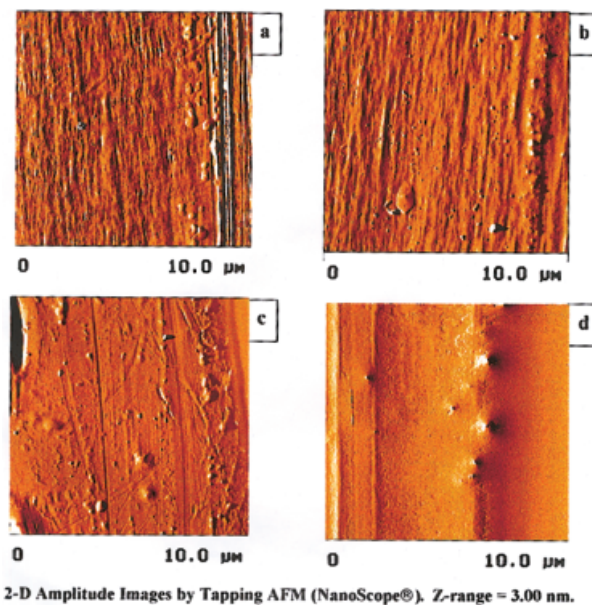


Figure 1 Two-dimensional amplitude images in the tapping mode of (a) unfinished and (b) finish-treated nylon-6 and (c) unfinished and (d) finish-treated PET fibers.

Table I Average Microroughness

Fiber Identification	Microroughness (nm)	
	10 × 10 μm ² Area	1 × 1 μm ² Area
Finish-free nylon-6	51.6 ± 20.8	10.3 ± 3.5
Finish-treated nylon-6	49.3 ± 23.5	15.6 ± 4.7
Finish-free PET	125.4 ± 42.8	17.7 ± 7.3
Finish-treated PET	78.5 ± 41.9	12.4 ± 6.6

Number of measurements per sample = 3/15.

saved images of the indentations (which were recorded in real time) after the experiment. From these images, features of interest can be calculated.

RESULTS AND DISCUSSION

Feasibility Study

An earlier feasibility study concerned with single indentations on single fibers, intended to establish the applicability of the technique, was followed by a more in-depth investigation applying multiple indentations along the lengths of several single fibers. The goal was to show that AFM measurements provide not only the distinguishing features of different types of fibers but also

the distinguishing features of unfinished and finish-treated specimens of the same fiber species.

The preliminary AFM study had shown opposite effects of a specific spin finish on the softening of nylon-6 and PET fibers. A more detailed study was necessary to establish the reliability of the earlier work. This study used a combination of three different signals—height, phase contrast, and amplitude—to characterize changes in the following characteristics of the fiber surface: the topography and morphology, microroughness, and total surface area as a result of treatment with a spin finish.

The core of this study, however, is the nanoindentation technique, which combined with profile scanning analysis and force–distance curves is able to measure changes in the microhardness of the fiber surface. Examples of single and multiple sequential indentations along the lengths of individual fibers, combined with profile scans, are discussed.

Characterization of the Fiber Surface

Detecting the Presence of a Spin Finish by Imaging the Height, Phase Contrast, and Amplitude

The amplitude images obtained in the tapping mode, shown in Figure 1(a–d), are the most demonstrative in displaying the presence of the spin finish on the treated nylon-6 and PET fibers. Spin-finish deposition on the treated nylon-6 fiber

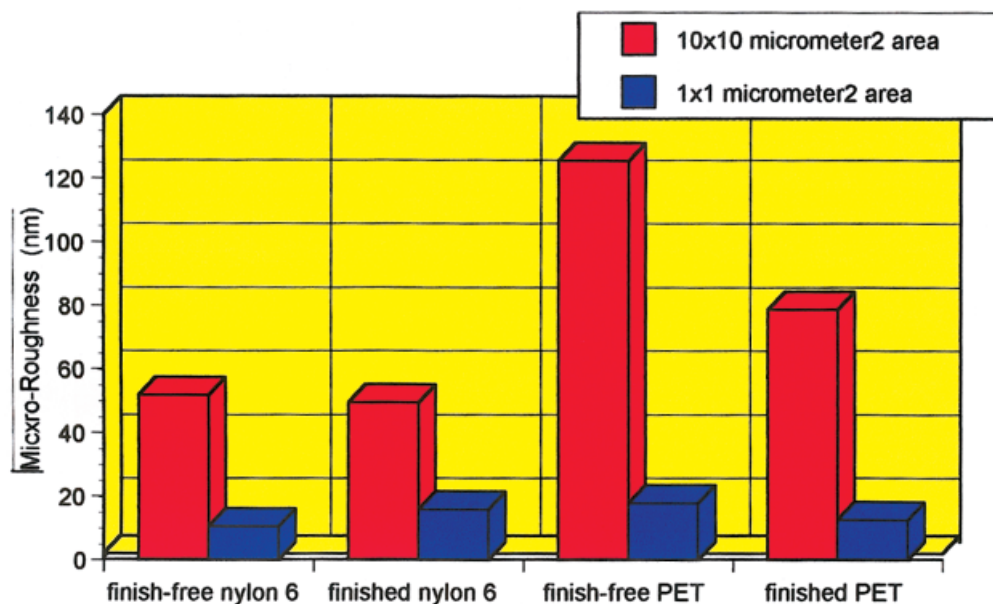


Figure 2 Changes in microroughness as a result of a spin finish.

Table II Average Total Surface Area Compared to the Measured Area of $10 \times 10 \mu\text{m}^2$

Fiber Identification	Total Surface Area (μm^2)/ $10 \times 10 \mu\text{m}^2$
Finish-free nylon-6	101.0 ± 0.4
Finish-treated nylon-6	108.2 ± 2.4
Finish-free PET	101.3 ± 0.7
Finish-treated PET	100.6 ± 0.4

Number of measurements = 3.

is hardly visible, and the appearance of the surface is probably indicative of finish absorption and swelling of the ridges [cf. Fig. 1(a,b)]. On the treated PET fiber, the thickness of the finish layer is significant [Fig. 1(d)]. This contrasting difference in finish deposition is reflective of different types of finish-fiber interactions in nylon and PET fibers.

Effect of Spin Finish on Microroughness

Microroughness measurements were made on 10×10 and $1 \times 1 \mu\text{m}^2$ areas of finish-free and finish-treated nylon-6 and PET fibers to establish differences between fiber types and changes in the coarse and fine surface structures due to treatment with a spin finish. Results are shown in Table I and Figure 2. The data and the graph indicate that the differences in the total micro-

roughness after finish treatments are large only for PET fibers. That there is no change for nylon probably suggests absorption of the finish by the softer nylon-6 surface. The differences are not statistically significant.

An approximately 30% decrease in microroughness in the finished specimens for the $10 \times 10 \mu\text{m}^2$ areas for PET fibers suggests that the surface is covered by a finish layer of about 45 nm. The microroughness data for the $1 \times 1 \mu\text{m}^2$ areas are less representative of the whole sample.

Effect of Spin Finish on Total Surface Area

AFM measurements of the total surface area (compared with the measured area of specific dimensions) provide additional parameters for establishing topographical and morphological changes in the fiber surface as a result of treatment with a spin finish. The areas used in this study measured $10 \times 10 \mu\text{m}^2$ in each case. As can be seen in Table II and Figure 3, AFM measurements show a significant increase in the total surface area for the nylon-6 fiber after the application of a spin finish, whereas the increase for the finished PET fibers is not significantly different. Comparing the amplitude images in Figure 1(a–d), we can see that the PET fiber is relatively smooth and has occasionally large asperities, which give it a higher roughness number. However, this does not contribute greatly to the surface area. When some of these asperities are filled

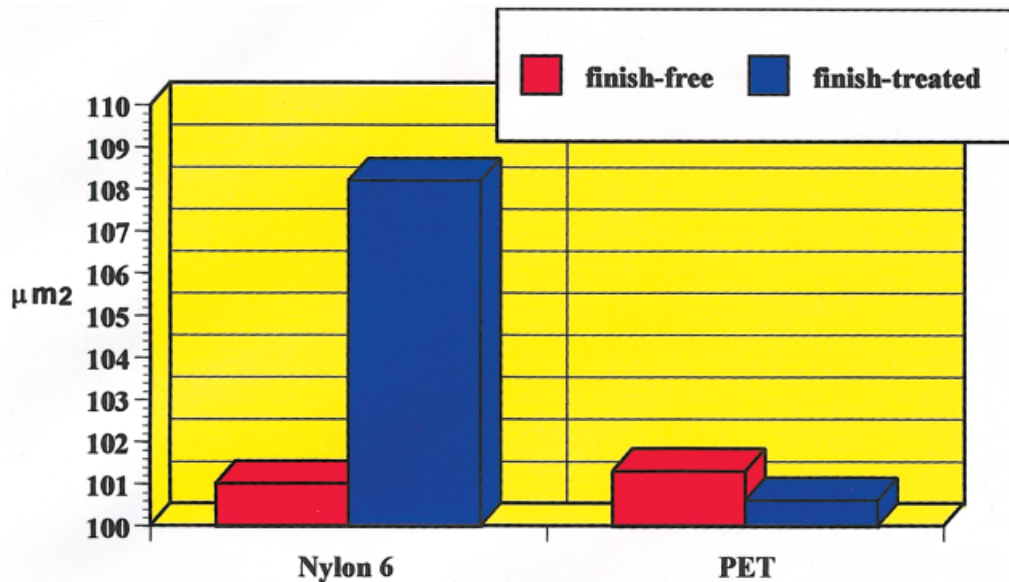


Figure 3 Difference between a measured area of $10 \times 10 \mu\text{m}^2$ and the total surface area of nylon-6 and PET fibers before and after the application of a spin finish.

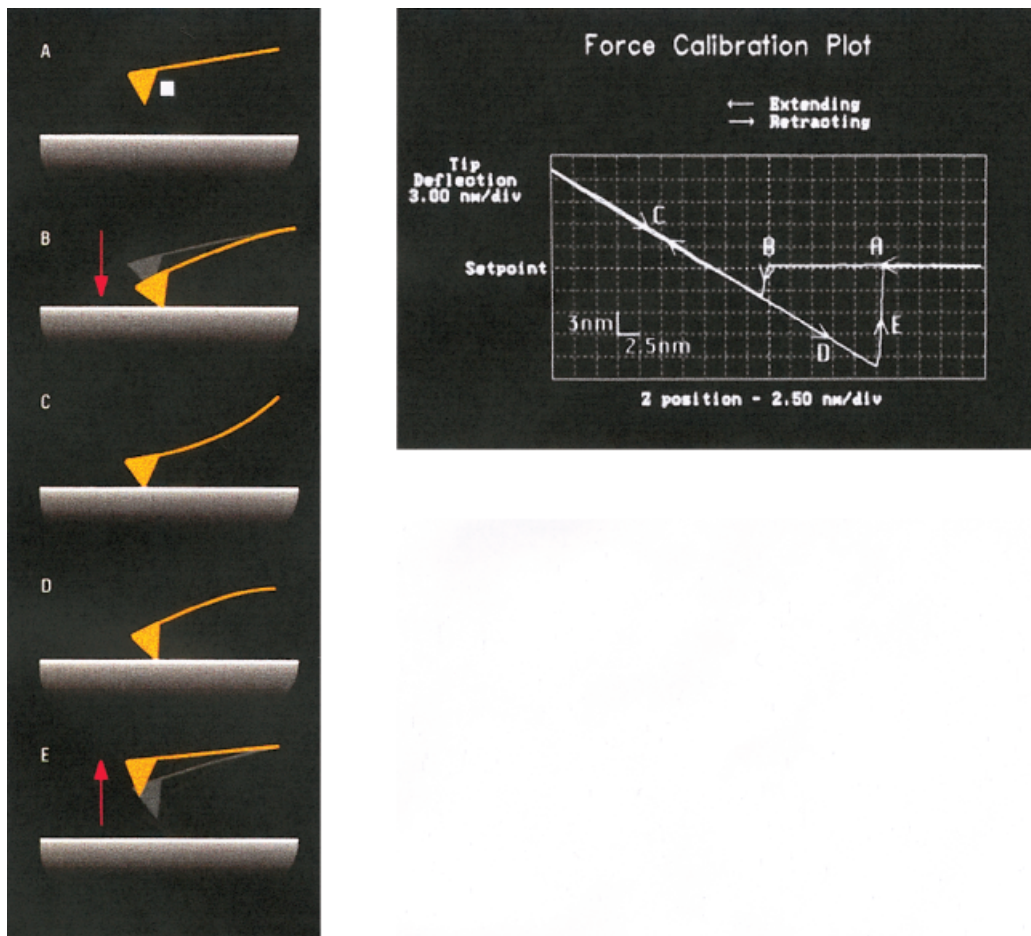


Figure 4 AFM measurements of cantilever–sample interactions (left) shown schematically at several points along the force curve (right): (A) approach, (B) jump to contact, (C) contact, (D) adhesion, and (E) pull-off or separation. (From Digital Instruments, Inc., Newsletter on Probing Nanoscale Forces with AFM.)

with the finish, the changes in the surface area are negligible. However, the nylon fiber has a relatively rough surface, and after the finish treatment, the asperities on the surface seem to swell [see Fig. 1(b)]. This can lead to a small but significant increase in surface area.

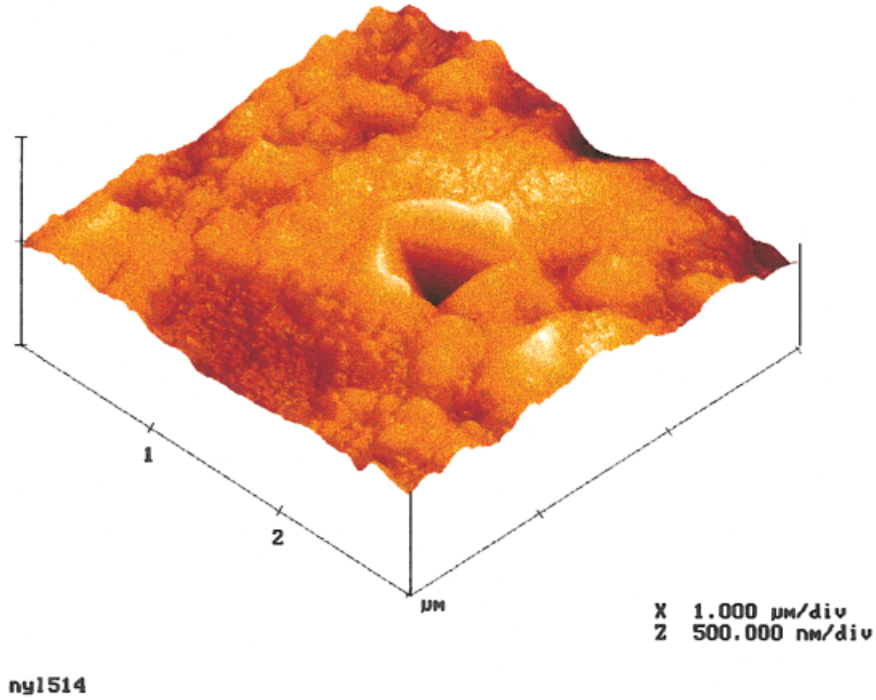
Effect of Spin Finish on Microhardness

Nanoindentation is a relatively new technique, which has been adapted by the AFM protocol to determine or compare the microhardness of surfaces of materials.^{1–3} In this case, nanoindentation measures the microhardness by indenting the fibers before and after treatment with a spin finish. Profile analysis measures the depth of the indentations on the saved images. The force distance curves reflect attractive, repulsive and adhesive forces between the probe tip and the sam-

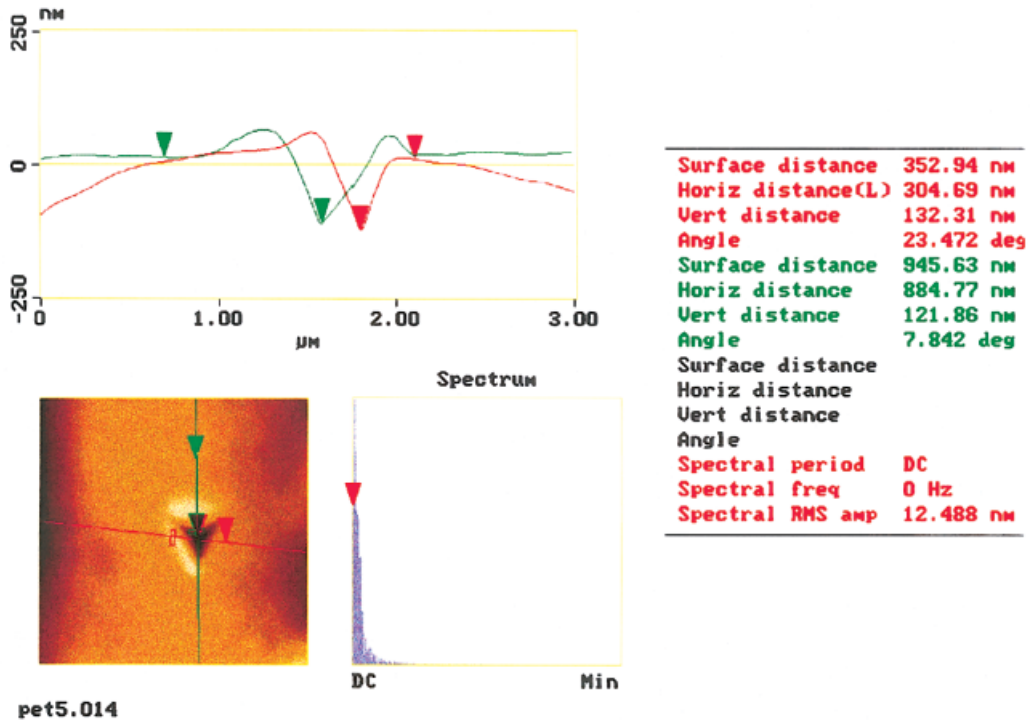
ple during indentation. This is schematically shown in Figure 4.

Nanoindentation at Low Forces, Profile Scanning Analysis, and Force–Distance Curves. In this study, a series of indentations were made axially along the length of the fiber. The indentations were separated from one another by several micrometers. The indentations in the upper fiber surface were made with a defined maximum force of 67 μN . The cantilever constant of the activated tip was 180 N/m.

Because it is very difficult to make quantitative statements about the microhardness of the upper surface layer of the fiber on the basis of the three-dimensional images alone, the corresponding profile scanning analysis and force curves play an important role in interpreting the data. For this part of the study, the profiles of the indentations

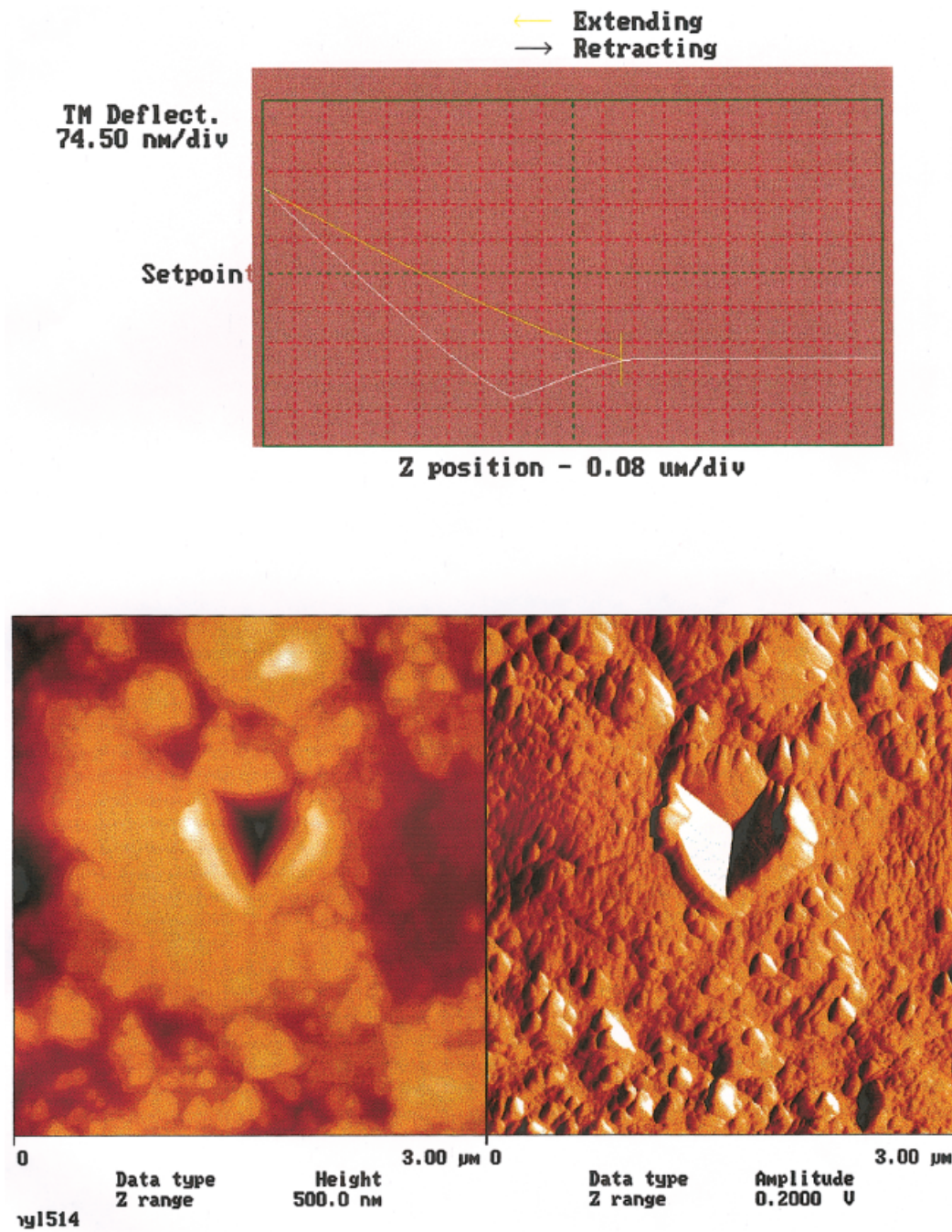


(a)



(b)

Figure 5 (a) Typical three-dimensional height profile of a nanoindentation (force of indentation = 67 μN) in a finish-free nylon-6 fiber, (b) corresponding profile scans measuring the depth [radially (red) and axially (green)] across the nanoindentation, and (c) representative force calibration curves (top) with corresponding height and amplitude images (bottom) of the nanoindentation.



(c)

Figure 5 (Continued from previous page)

were scanned in both the radial (red) and axial (green) direction of the fiber, thereby yielding two profile scans per image. On the basis of the deformation of the crater rim and the curvature of the fiber, the measurements along the length of the fiber are preferable. Representative three-dimen-

sional height profiles of the nanoindentations with the corresponding profile scans of the indentations, as well as the relevant force calibration curves with the corresponding height and amplitude images of the indentations of the untreated and finish-treated fibers, are shown in Figures

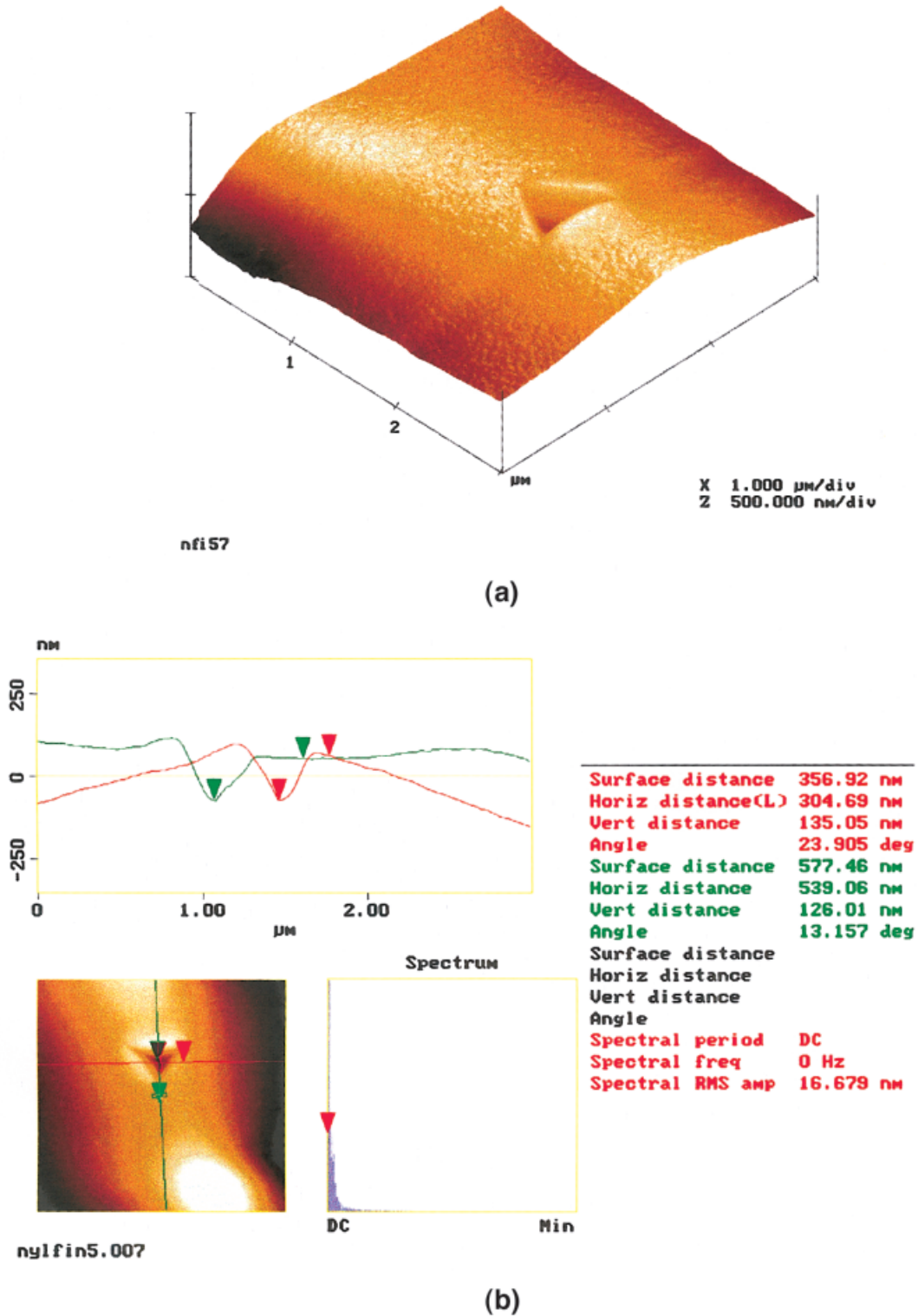


Figure 6 (a) Typical three-dimensional height profile of a nanoindentation (force of indentation = $67 \mu\text{N}$) in a finish-treated nylon-6 fiber, (b) corresponding profile scans measuring the depth [radially (red) and axially (green)] across the nanoindentation, and (c) representative force calibration curves (top) with corresponding height and amplitude images (bottom) of the nanoindentation.

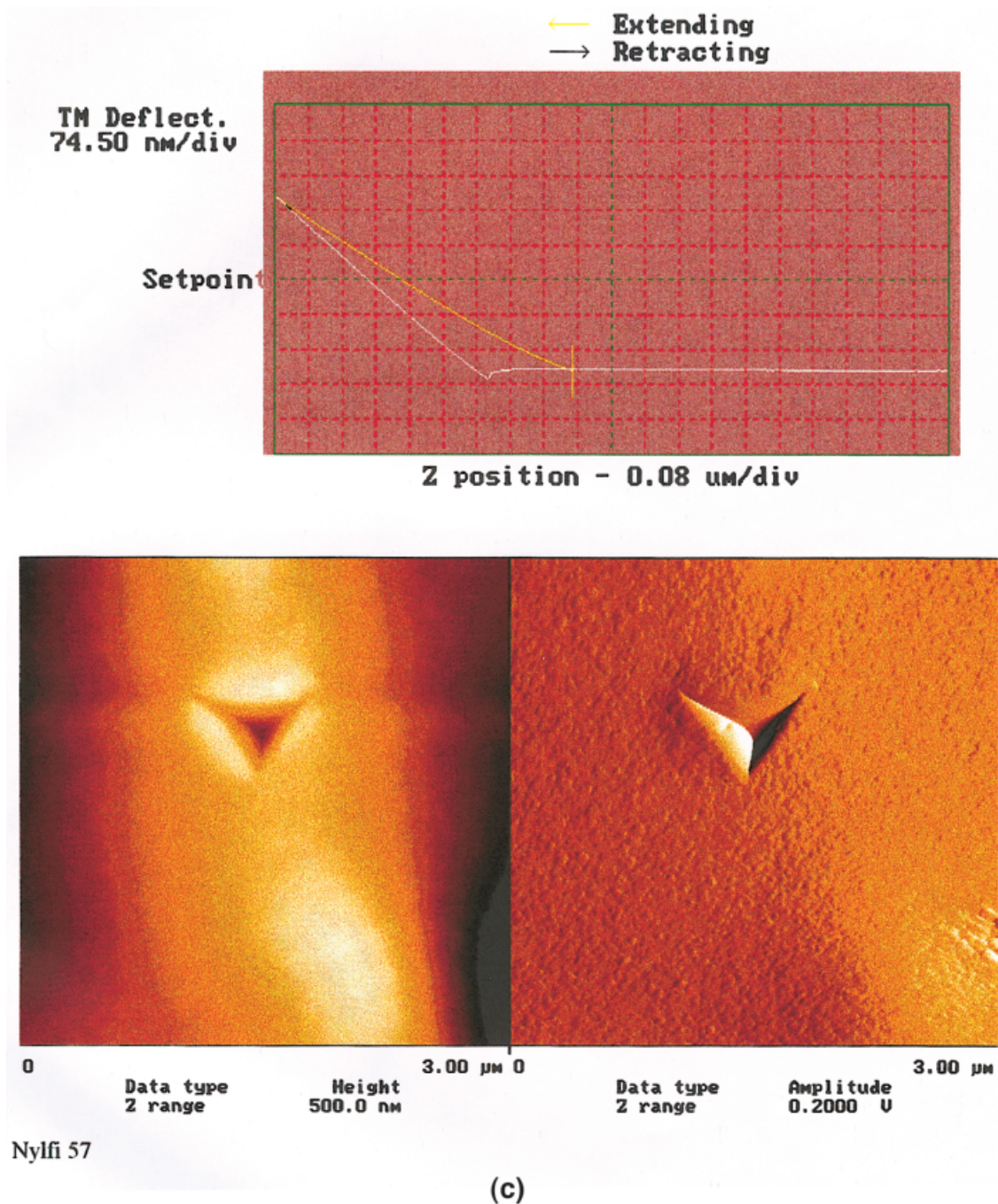


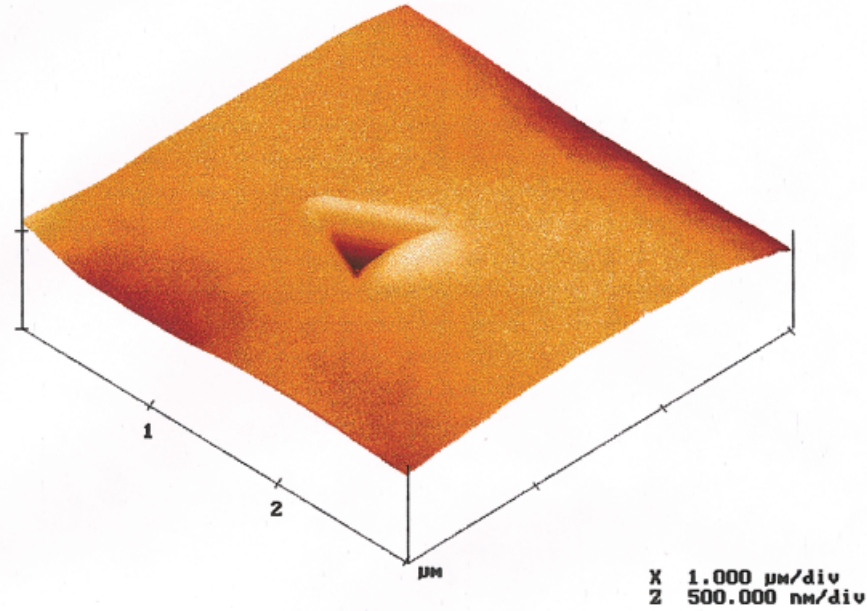
Figure 6 (Continued from previous page)

5(a-c), 6(a-c), 7(a-c), and 8(a-c). The results of the depth measurements of the indentations are summarized in Table III.

The appearance of the indentation is shown in Figure 5(a). The axial and radial profile scans of the indentation and the direction of the measurement are shown in Figure 5(b). The picture of the indentation shows the difficulty of indenting a

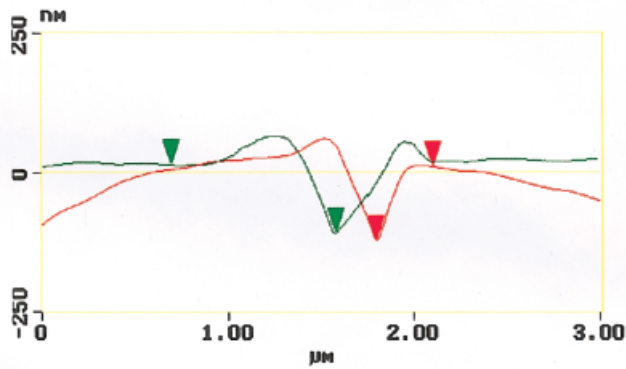
curved surface. Obviously, the indenter slipped to one side, leading to an unsymmetrical indentation. This can be seen clearly from the profile scan in Figure 5(b) (green). Therefore, it is important to indent exactly on top of the dome of the fiber. The force curve (top) and the amplitude image (bottom, right) are shown in Figure 5(c).

The force curve for finish-free nylon-6 fibers

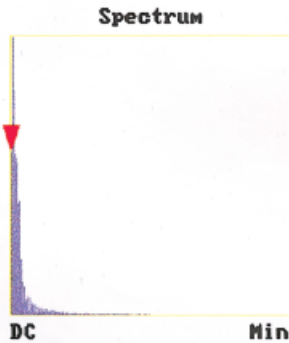
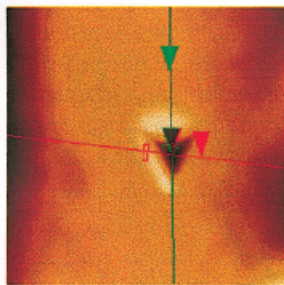


Pet fin-free 5.14

(a)



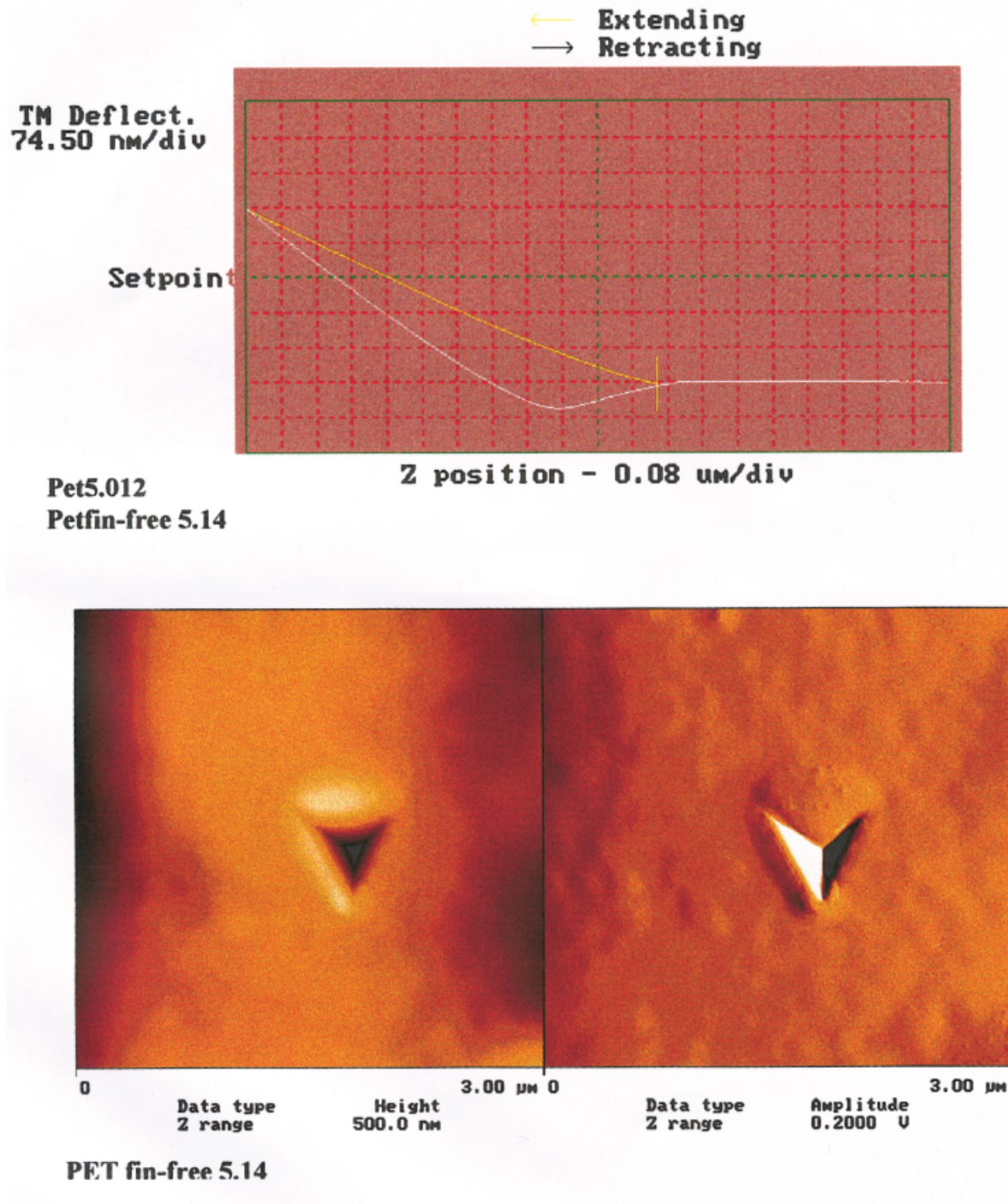
Surface distance	352.94 nm
Horiz distance(L)	304.69 nm
Vert distance	132.31 nm
Angle	23.472 deg
Surface distance	945.63 nm
Horiz distance	884.77 nm
Vert distance	121.86 nm
Angle	7.842 deg
Surface distance	
Horiz distance	
Vert distance	
Angle	
Spectral period	DC
Spectral freq	0 Hz
Spectral RMS amp	12.488 nm



Pet fin-free 5.14

(b)

Figure 7 (a) Typical three-dimensional height profile of a nanoindentation (force of indentation = 67 μ N) in a finish-free PET fiber, (b) corresponding profile scans measuring the depth [radially (red) and axially (green)] across the nanoindentation, and (c) representative force calibration curves (top) with corresponding height and amplitude images (bottom) of the nanoindentation.



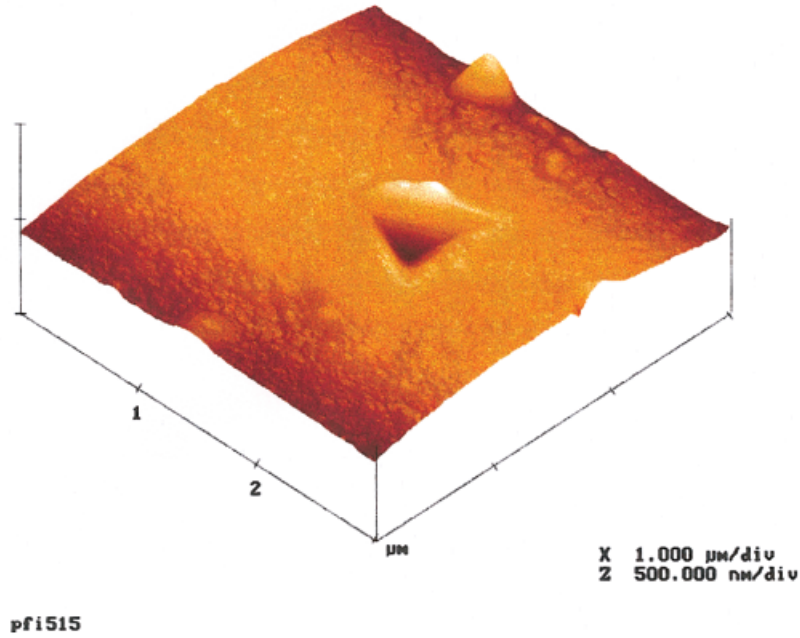
(c)

Figure 7 (Continued from previous page)

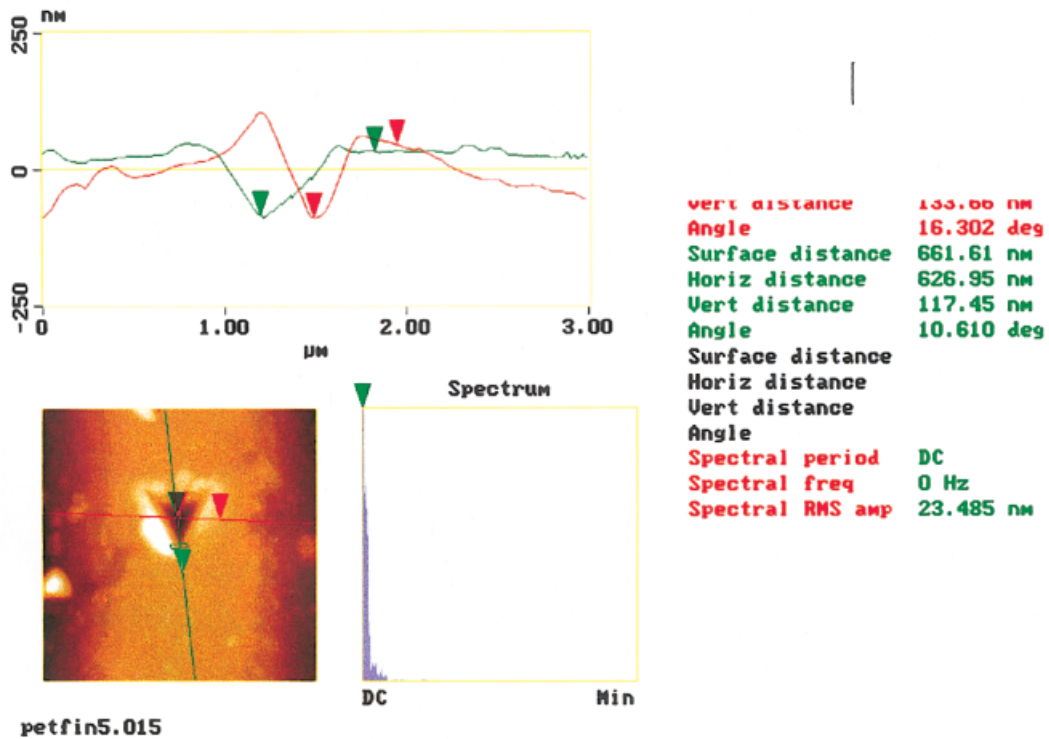
[Fig. 5(c)] shows that the material deforms plastically and adheres to the indenter. The magnitude of the adhesion force is around 16.1 μN. The force curve for the finish-treated fiber also shows plastic deformation (although less compared with

that of the finish-free fiber) with no adhesion. The absorbed finish lubricates the indenter surfaces.

Comparisons of the profile scans of Figure 5(b) and Figure 6(b) show that the depths of the indentations on finish-treated fibers are lower. The



(a)



(b)

Figure 8 (a) Typical three-dimensional height profile of a nanoindentation (force of indentation = $67 \mu\text{N}$) in a finish-treated PET fiber, (b) corresponding profile scans measuring the depth [radially (red) and axially (green)] across the nanoindentation, and (c) representative force calibration curves (top) with corresponding height and amplitude images (bottom) of the nanoindentation.

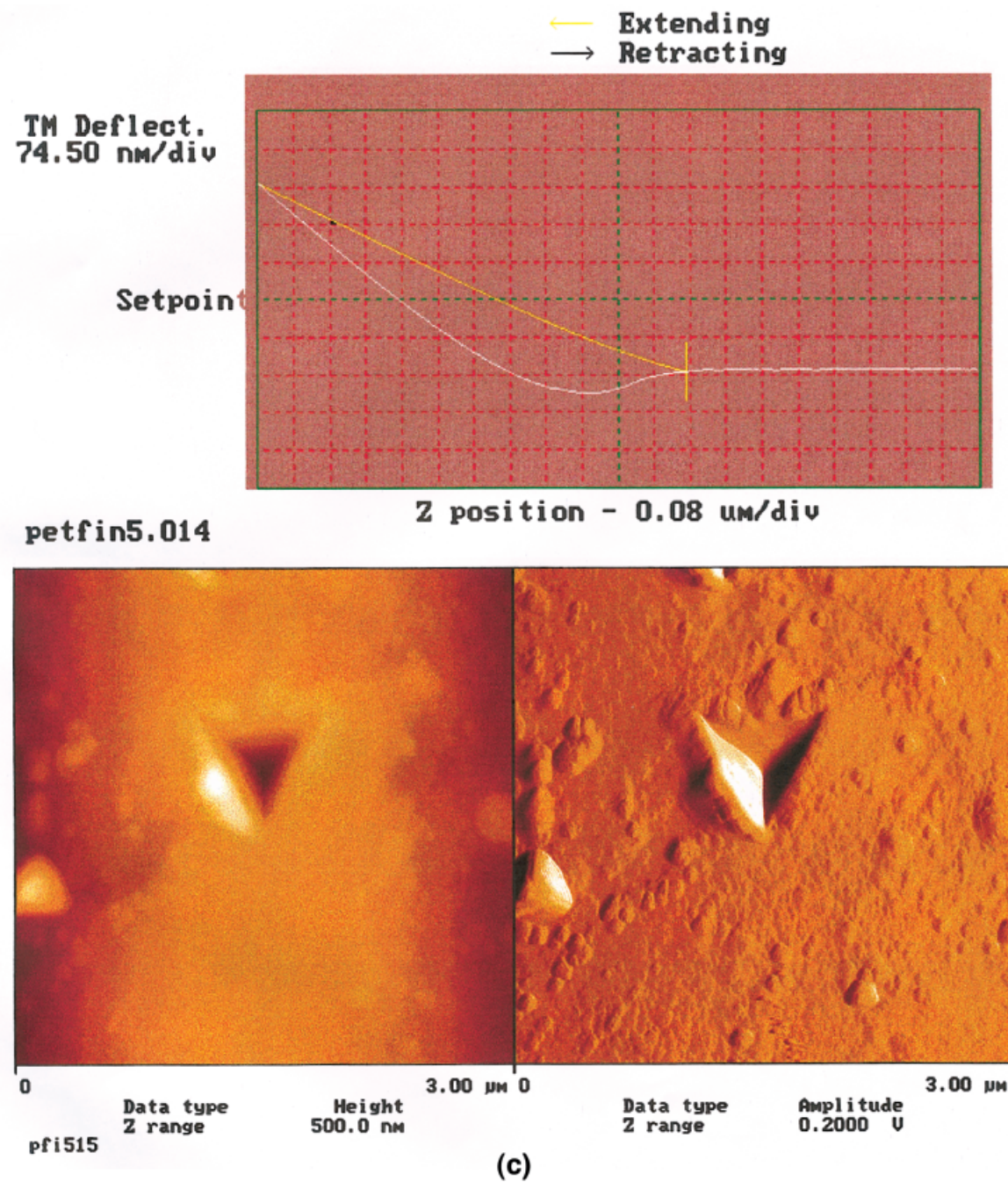


Figure 8 (Continued from the previous page)

indentations are also more rounded. This shows that the material has been plasticized to a rubbery state, which recovers after deformation. This is also supported by the amplitude images in Figures 5(c) and 6(c); the apex of the latter is flat compared with that of the former. This shows that the finish plasticizes the polyamide into a slightly more elastic material, which recovers af-

ter indentation. This results in a lower area for the hysteresis loop in Figure 6(c) than in Figure 5(c).

Similar indentation data for finish-free and finish-treated PET fibers are shown in Figures 7(a-c) and 8(a-c), respectively. In this case, the force curves for the two types of fiber are very similar, showing that the effect of the finish is

Table III Average Indentation Depth of Finish-Free and Finished Fibers

Fiber Identification	Depth of Indentation (nm)	
	Radial (67 μN)	Axial (67 μN)
Finish-free nylon-6 ^a	132.3 \pm 12.1	142.2 \pm 20.9
Finish-treated nylon-6 ^b	106.1 \pm 32.8	125.8 \pm 34.7
Finish-free PET ^a	144.3 \pm 8.3	133.6 \pm 9.5
Finish-treated PET ^b	131.8 \pm 16.9	117.1 \pm 12.6

^a Averages were obtained from six individual measurements.

^b Averages were obtained from three individual measurements.

negligible. As for nylon-6, adhesion ($\sim 12 \mu\text{N}$) is reduced to about $7 \mu\text{N}$ as a result of the finish treatment.

Profile scans [Figs. 7(b) and 8(b)] of the PET fibers show rounded indentations in the finish-treated specimen (not as much as in nylon-6); this is further supported by the amplitude images shown in Figures 7(c) and 8(c). The apex of the triangular pyramid for the finish-treated fiber is slightly flatter than that of the finish-free fiber.

The numerical data on the depth of indentations is shown in Table III. A trend shows that the finish-treated fiber gives an indentation shallower than the finish-free fiber. The difference is not statistically significant. The physical observations made earlier support the trend.

Nanoindentations at High Forces and Profile Scanning Analysis. Five sequential indentations were made in the upper fiber surface with a special diamond probe tip with a defined force of $147 \mu\text{N}$. This selected force was 2 times greater than the force applied earlier ($67 \mu\text{N}$).

To be able to make quantitative statements about the microhardness of the upper surface layer of the fiber, we used the nanoindentations (three-dimensional profiles) in conjunction with the profile scanning analysis. The depth of the indentations was recorded in real time. This is important because it does not account for the recovery of the substrate. Figures 9(a,b) and 10(a,b) are typical examples of the five sequential nanoindentations and corresponding profile scans of the finish-free and finish-treated nylon-6 fibers, respectively. Figures 11(a,b) and 12(a,b) give representative examples of the five sequential nanoindentations and corresponding profile scans

of unfinished and finish-treated PET fibers, respectively.

A summary of the microhardness measurements (depth of nanoindentation) made by the cross-sectional scans on the saved, real-time images of the nanoindentations in finish-free and finish-treated nylon-6 and PET fibers is given in Table IV and Figure 13.

Nanoindentation and Microhardness

Although this work was initiated to study the microhardness of nylon and PET fibers and the effect of finish lubricants on the surface properties of the polymer, the results in this study suggest that the link between indentability and hardness for a polymeric material, especially in the presence of a plasticizing lubricant, may be a tenuous one.

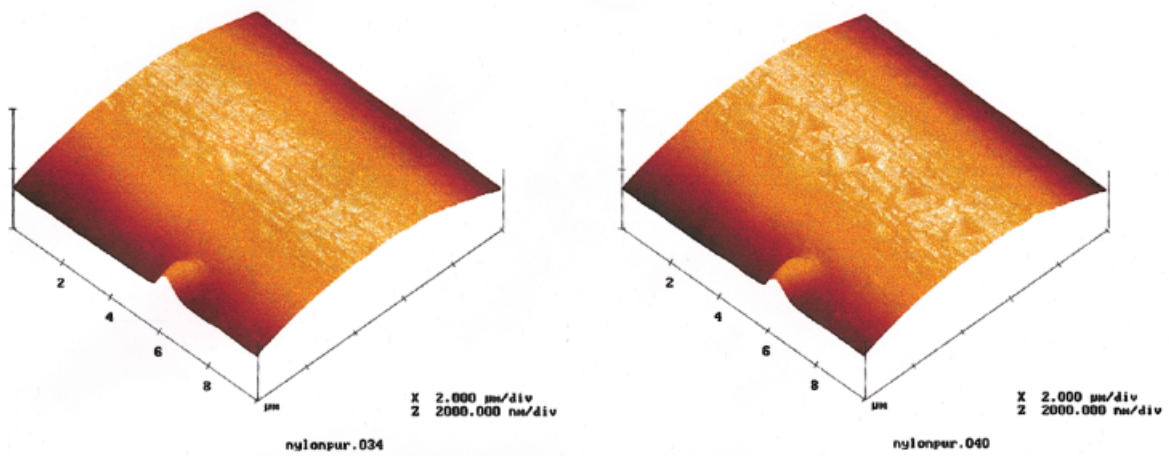
In this study, we could not differentiate between the behavior of nylon-6 and PET with indentation at low forces. The differences in indentation depths were not significant (Table III).

At high normal forces, however, we can distinguish between the behavior of nylon-6 and PET before and after the application of the finish. The indentation data are statistically significant. Therefore, it is important to select a force range that is commensurate with the material properties.

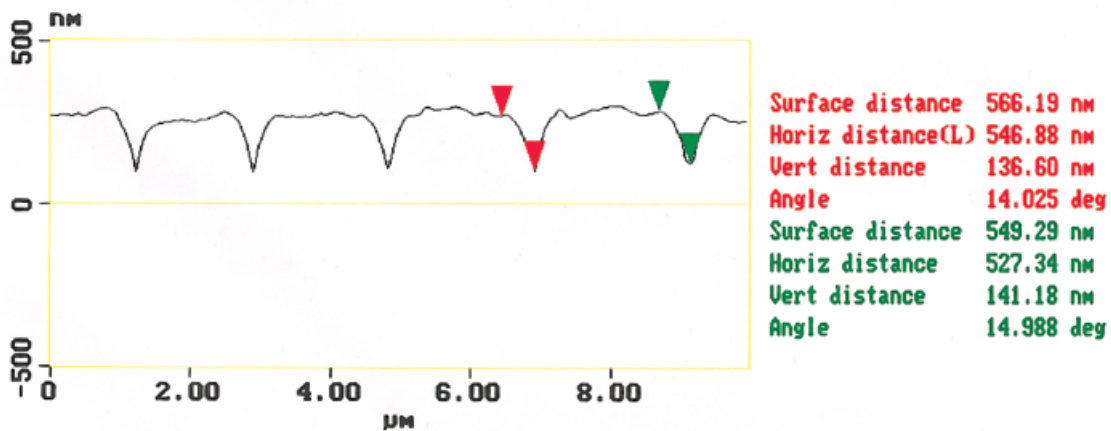
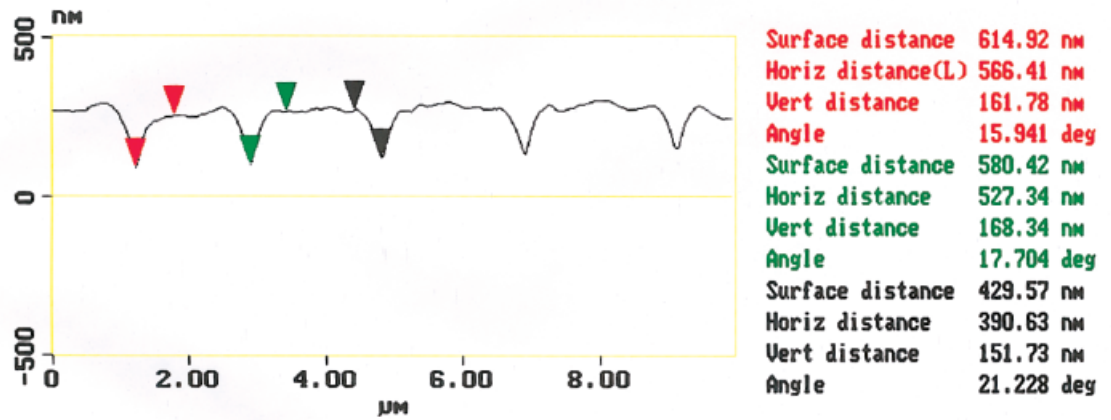
At a high force of indentation, the depth of indentation decreases in nylon-6 but increases in PET as a result of the finish lubricant. In the finish-free condition, PET is harder than nylon-6 at ambient humidity. This is supported by the indentation data. Treatment with the finish lubricant seems to soften both fibers to different degrees. However, we believe that plasticized nylon-6, because of its characteristic rubbery nature, pushes back on the indenter and, therefore, results in a lower indentation depth. PET is not as well plasticized by the finish lubricant as nylon-6 and so does not adhere to the indenter as well as nylon-6 and also deforms plastically. It is indeed possible that the finish lubricant acts as a lubricant on the indenter and, therefore, results in a greater depth of indentation. It may be incorrect to conclude that the finish lubricant makes nylon harder and PET softer on the basis of only the depth of indentation.

Relevance to Fiber Processing

The softening effect observed for both nylon and PET fibers as a result of interactions with the



(a)



(b)

Figure 9 (a) Typical three-dimensional height profiles of a finish-free nylon-6 fiber before and after five sequential nanoindentations (force of indentation = 147 μ N) and (b) corresponding cross-sectional scans measuring the depth of the nanoindentations.

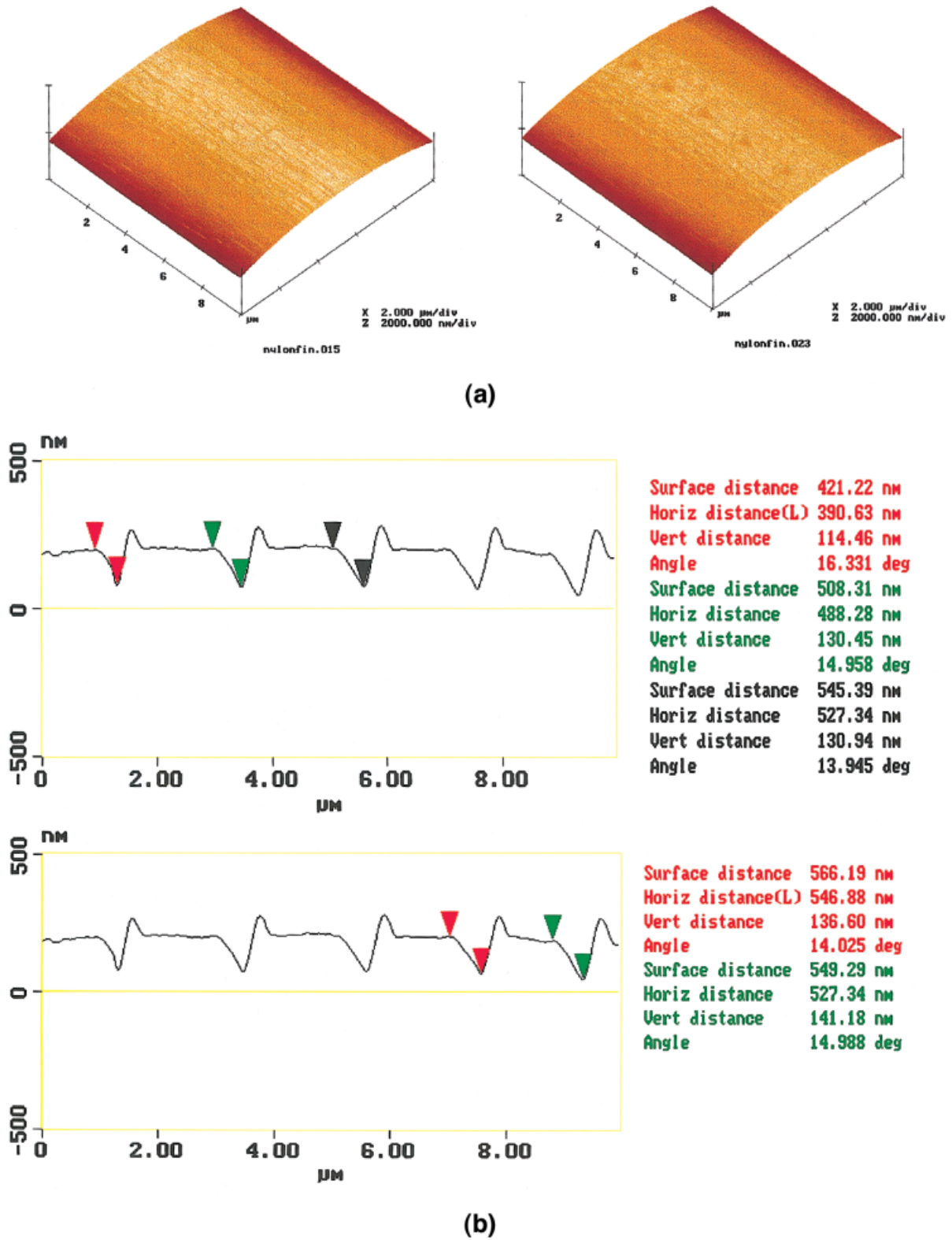


Figure 10 (a) Typical three-dimensional height profiles of a finish-treated nylon-6 fiber before and after five sequential nanoindentations (force of indentation = 147 μN) and (b) corresponding cross-sectional scans measuring the depth of the nanoindentations.

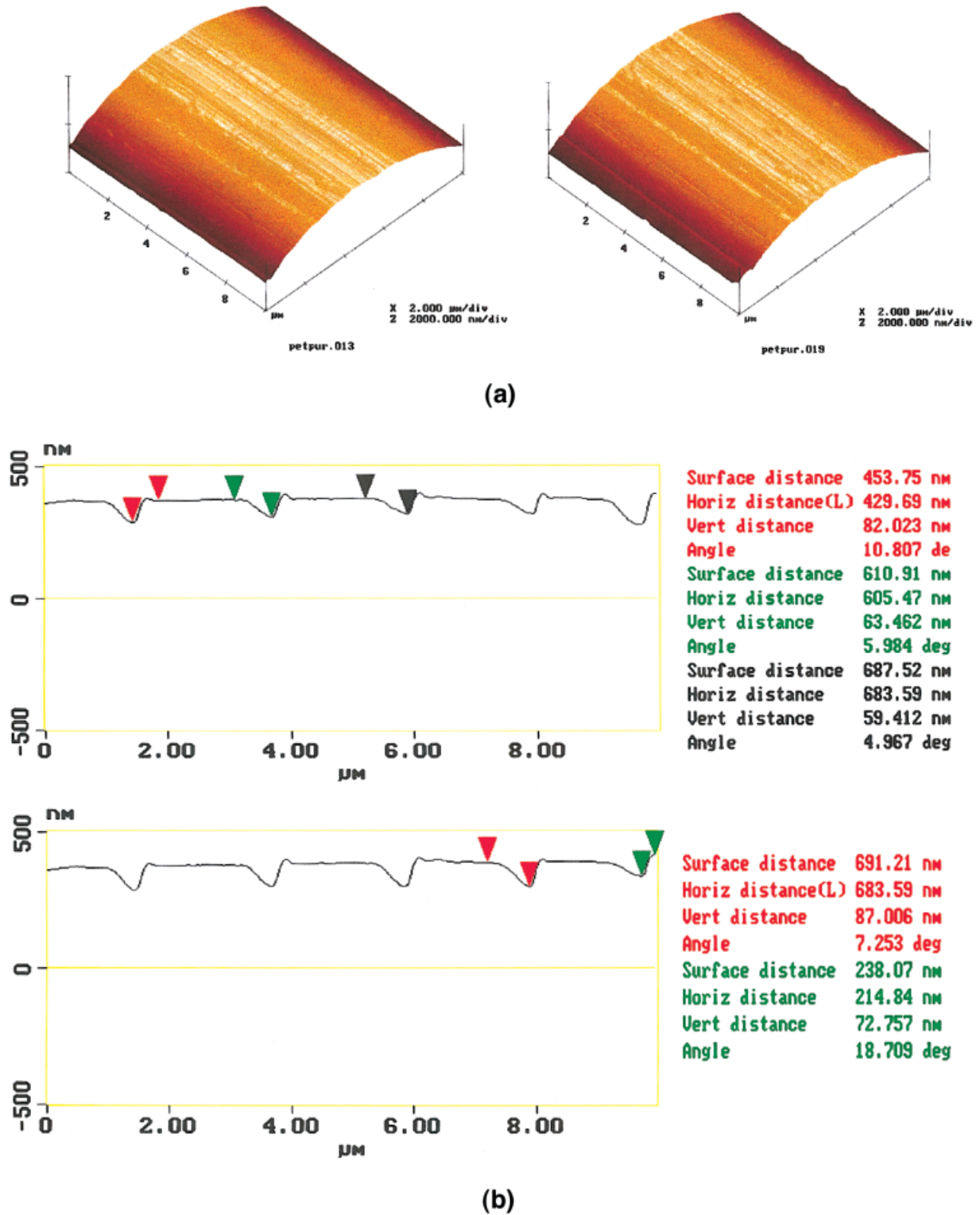


Figure 11 (a) Typical three-dimensional height profiles of a finish-free PET fiber before and after five sequential nanoindentations (force of indentation = 147 μ N) and (b) corresponding cross-sectional scans measuring the depth of the nanoindentations.

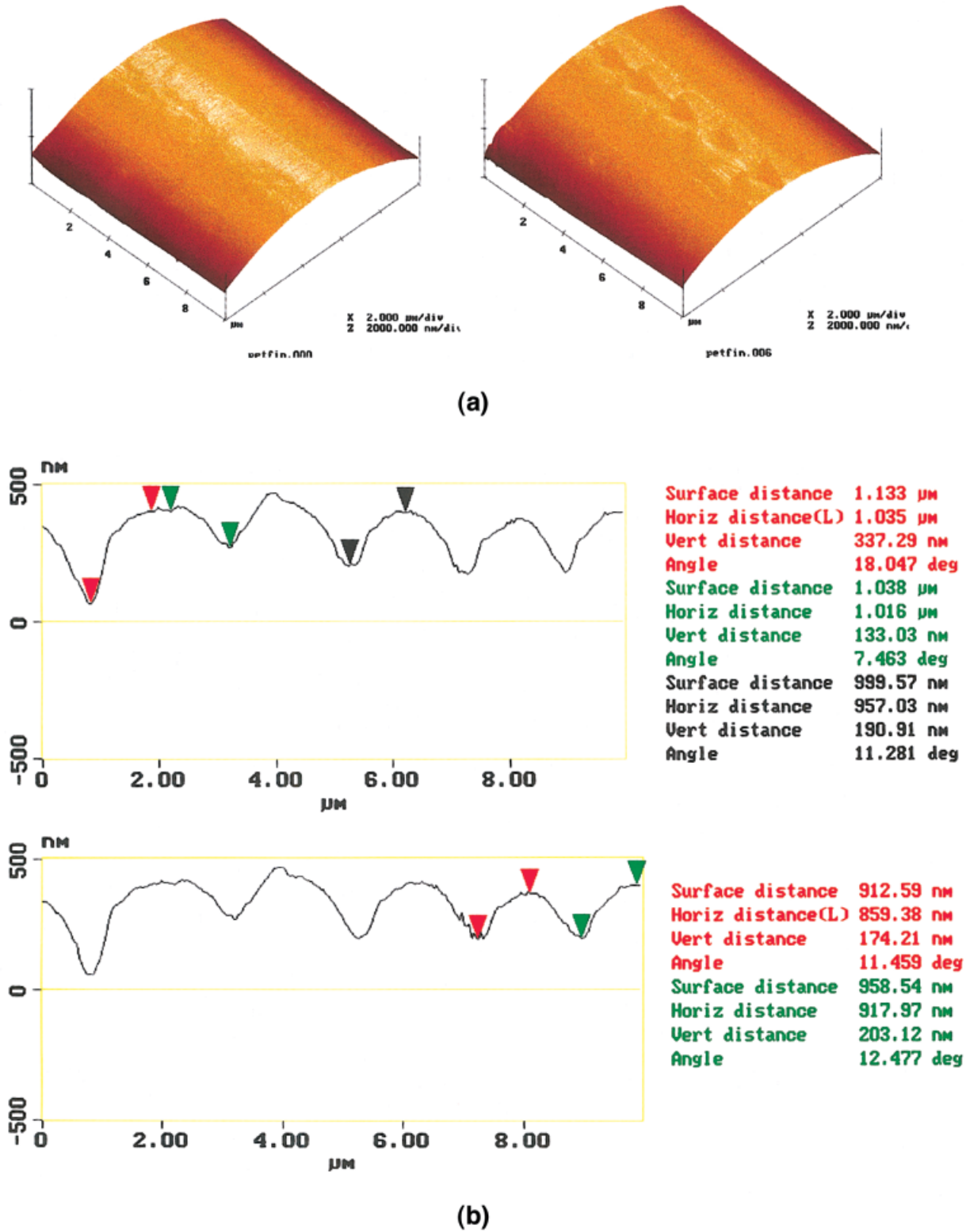


Figure 12 (a) Typical three-dimensional height profiles of finish-treated PET fiber before and after five sequential nanoindentations (force of indentation = 147 μN) and (b) corresponding cross-sectional scans measuring the depth of the nanoindentations.

Table IV Average Microhardness and Depth of Indentation from Cross-Sectional Scans

Fiber Identification	Depth of Nanoindentation (nm)
Finish-free nylon-6	162.2 ± 7.4
Finish-treated nylon-6	130.7 ± 10.1
Finish-free PET	72.9 ± 11.8
Finish-treated PET	207.7 ± 77.1

Number of measurements = 5.

spin finish lubricant has important consequences for fiber processing. Softening the surface of a fiber generally leads to an increase in fiber friction against metal surfaces, which are used in processing. This can lead to fiber breakage and adhesion, affecting productivity and the quality of the product.

In the fiber trade, especially for synthetic fibers, packages of yarn often remain in the warehouse up to 3 months. During this period, the water from the spin finish evaporates, and the lubricants and surfactants redistribute by spreading. Although finish lubricants (EO/PO) are not supposed to dissolve in the fiber, their chemistry and prolonged contact lead to interactions with the fiber. This can plasticize the surface layers of fibers, which, in turn, can have an adverse effect on fiber friction against other surfaces.

We made an attempt to evaluate this effect on nylon-6 and PET fibers of textile denier (20–30 μm in diameter). Friction forces of untreated and

finish-treated fibers against a stainless steel wire were measured at three different normal forces ($N = W \sin \theta$) through changes in the angle θ .

The device, schematically shown in Figure 14, is used on an Instron machine (Instron Company, Canton, MA) to measure the friction forces. The fiber is mounted vertically on the Instron load cell, and the stainless steel wire is mounted on the bow, which is fixed to the micrometer gauge. The vertical fiber and the horizontal wire are brought into contact with each other by the micrometer gauge being moved. θ is adjusted by the stainless steel wire being pushed against the vertical fiber. The larger θ is, the higher the normal force is. Friction force is measured by the cross-head being moved down when the stainless steel wire slides against the vertical fiber.

After the application of the finish lubricant, the specimens were stored for different lengths of time before the friction measurements were made. Several specimens were used for each condition. Measurements were not repeated on any specimen; instead, new specimens were used for each storage time. Friction forces for PET and nylon-6 fibers are shown in Figures 15 and 16, respectively, at three different normal forces (0.31, 0.51, and 0.8 g). In the graph, the tension applied to the fiber is given as 3, 5, or 8 g. Each value is an average of measurements from 10 specimens. The maximum storage time was 3 months after application of the finish lubricant.

For both nylon and PET fibers, friction forces go down immediately after the finish application. The decrease in nylon is slightly greater than in PET. This may suggest a faster interaction be-

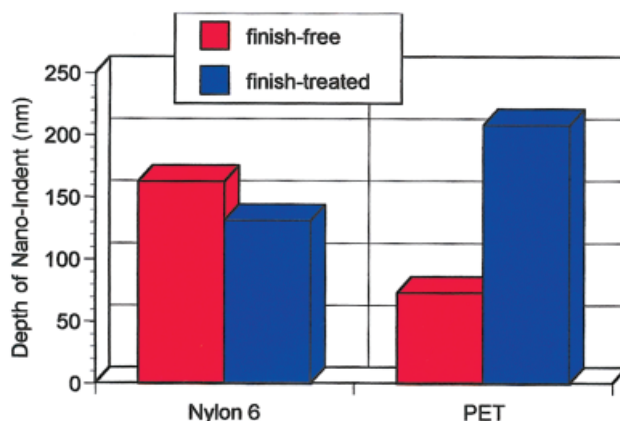


Figure 13 Effect of the spin finish on the microhardness of nylon-6 and PET fibers. Nanoindentations were made with a defined force of 147 μN .

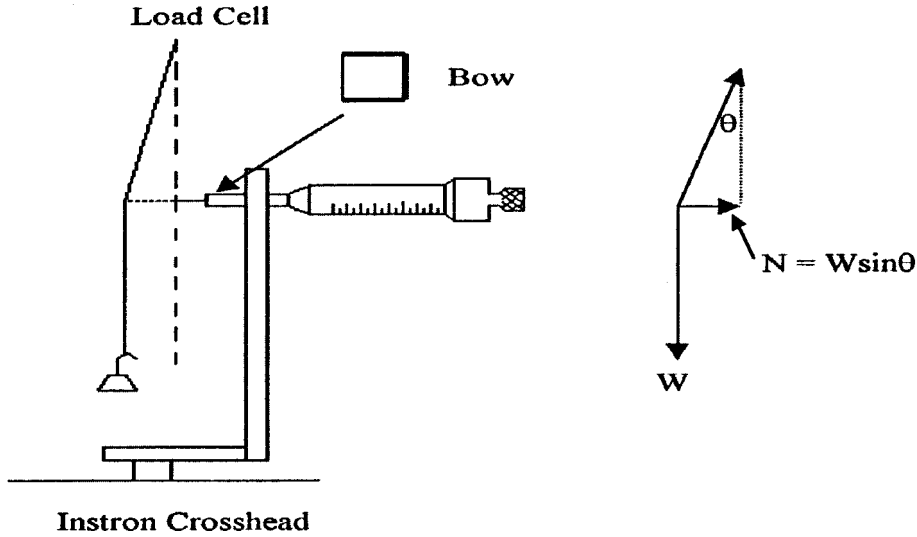


Figure 14 Schematic drawing of the single-fiber friction apparatus.

tween the finish and fiber leading to plasticization. This will reduce the shear strength of the material. Because the friction force (f) is a product of the area of real contact (A) and the shear strength of the junctions (s ; i.e., $f = As$),⁴ a larger decrease for nylon is likely to be due to a decrease in the shear strength of the interface. The lubricating effect of the liquid film is present in both

cases. The reduction in shear strength is likely to be less for PET.

The data also show that the effect of softening on friction is very low at low normal forces (3 g). However, at higher normal forces, the softened interfacial layer is sheared, and this gives rise to energy dissipation and an increase in friction. The data clearly show that the interaction of the

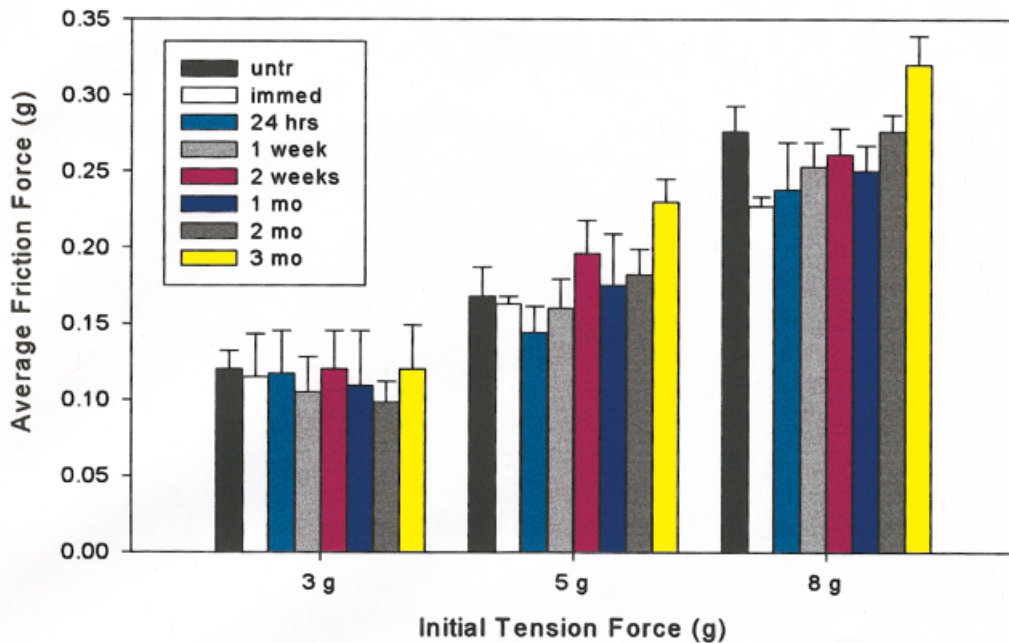


Figure 15 Average friction force for PET fibers as a function of the initial tension force and fiber-finish interaction time.

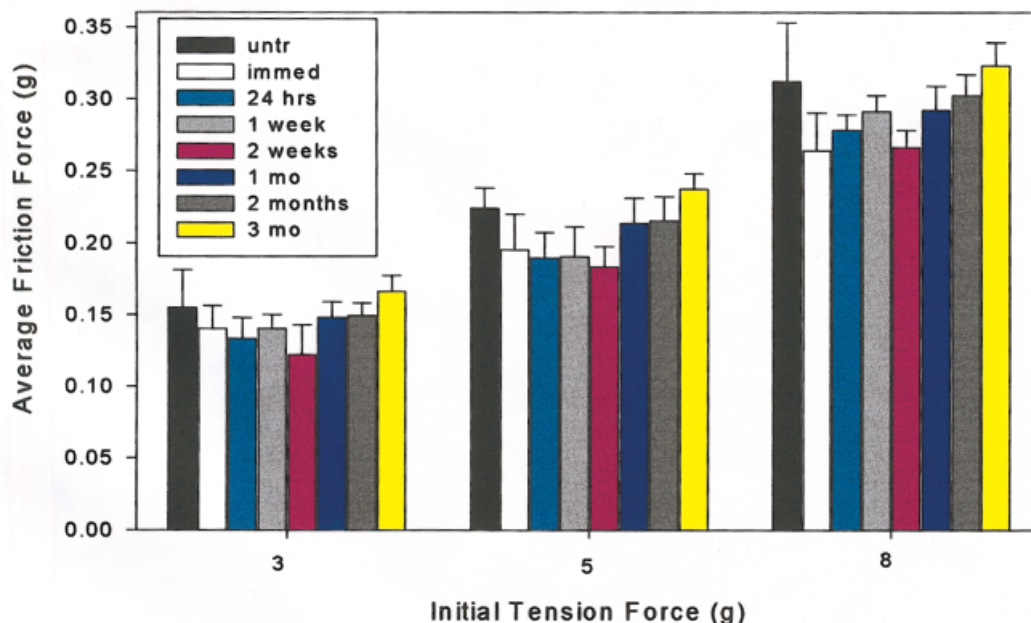


Figure 16 Average friction force for nylon-6 fibers as a function of the initial tension force and fiber–finish interaction time.

finish lubricant with the polymer over long periods of time gives rise to an increase in fiber friction against a hard metal surface. The increase is greater for PET than for nylon.

CONCLUSIONS

These investigations show that AFM measurements are capable of distinguishing not only different types of fibers but also unfinished and finish-treated specimens of the same fiber species. The various AFM techniques clearly establish different effects of a specific spin finish on the surfaces of different polymeric substrates. This study shows that AFM investigations with nanoindentation are useful in establishing finish-induced modifications in micromechanical properties (hardening or softening) of a fiber surface.

The outcome of this study indicates that EO/PO finish components have a greater softening effect on the surface of nylon-6 fibers than on those of PET. The effect seems to be one of plasticization of the finished fiber surface, which acquires some elasticity so that the deformed surface resists indentation and recovers better than the finish-free surface. This is what leads to the differences in indentation depths for the untreated and finish-treated fibers, as well as the differences in the recovery behaviors of nylon and PET.

Although nanoindentation is a difficult technique on curved fiber surfaces, the results obtained in this study show that useful information about the effects of interacting liquids on fibers of textile denier can be obtained.

Fiber friction measurements corroborate the nanoindentation studies, thereby establishing a link between basic and applied research. The method will be useful in selecting proper components for the formulation of a spin finish.

REFERENCES

1. VanLandingham, M. R.; Knight, S. H.; Palmese, G. R.; Eduljee, R. F.; Gillespie, J. W., Jr.; McCullough, R. L. In *Materials Research Society Proceedings*; Cammarata, R. C., Chason, E. A., Einstein, T. L., Williams, E. D., Eds.; Materials Research Society: Warrendale, PA, 1997; Vol. 440, p 195.
2. VanLandingham, M. R.; Knight, S. H.; Palmese, G. R.; Bogetti, T. A.; Eduljee, R. F.; Gillespie, J. W., Jr. In *Materials Research Society Proceedings*; Briant, C. L., Carter, B., Hall, E. L., Eds.; Materials Research Society: Warrendale, PA, 1997; Vol. 458, p 313.
3. VanLandingham, M. R.; Dagastine, R. R.; Eduljee, R. F.; McCullough, R. L.; Gillespie, J. W., Jr. *Compos A* 1999, 30, 75.
4. Bowden, F. P.; Tabor D. *The Friction and Lubrication of Solids*; Oxford University Press: London, 1964; Part 2, p 220.